Towards landmarks prediction with Deep Network

Van Linh Le[1,3], **Marie Beurton-Aimar**[1], **Akka Zemmari**[1], **Nicolas Parisey**[2]

[1]LaBRI - CNRS 5800 Bordeaux University, France, van-linh.le/beurton/zemmari@labri.fr
[2]IGEPP - INRA 1349, France, nparisey@rennes.inra.fr
[3]ITDLU - Dalat University, Vietnam, linhlv@dlu.edu.vn

Keywords: Landmarks, convolutional neural networks, fine-tuning, recogntion, morphometry analysis.

Abstract

Morphometry landmarks are used in many biological applications. Mostly, the landmarks are defined manually or semi-automatically by applying image processing techniques. In recent years, Deep Learning is known as a solution to achieve image analysis tasks such as classification, recognition, or face detection. In this context, we present a Convolutional Neural Network (CNN) model to predict landmarks on 2D anatomical images, specifically beetle's images. The dataset includes the images of collecting from 293 beetles. For each beetle, 5 images are available corresponding to *head, pronotum* and *body* parts. For each part, a set of manual landmarks has been positioned by an entomologist. In this work, we have focused on prediction of pronotum landmarks. The proposed CNN model is designed from an *elementary block* of three layers: convolution, pooling, and dropout. The network is trained in two different ways: from scratch or after a step of fine-tuning. The fine-tuning parameters are obtained by training on all parts of beetles before to be applied to the pronotum. The quality of predicted landmarks is evaluated by calculating the distance in pixels between the coordinates of the predicted and manual landmarks which are considered as the ground truth. The obtained results by applying fine-tuning steps are considered to be statistically good enough to replace the manual ones for the different morphometry analysis.

1 Introduction

Morphometrics landmarks (or point of interest) are important features in many biological investigations. They are used to analyze the shape of biological organs or organisms. These shape analyses are mainly based on metrics extractions from landmarks coordinates. Depending on the anatomical part, the number of landmarks may vary. As well as their position can be stayed on the edges or inside the anatomical part. For example, the landmarks on Drosophila wings [1] are inside the wings, near veins, but the landmarks on human ear [2] can be located at the ear edge or inside the pinna. Currently, the landmarks are set manually by the entomologist, one can note that this work is time-consuming and difficult to reproduce when users change. Therefore, a method that proposes automatically the coordinates of landmarks could be a concern.

In image processing, segmentation is most often the first and the most important step. This task remains a bootleneck to compute features of an image. In some cases, the object of interest is easy to extract and can be analyzed with the help of a lot of very well-known image analysis procedures. In a previous study [3], we have analyzed two parts beetle mandibles. These parts are pretty easy to segment (at least with an enough good quality for our needs). In this work, we have applied a set of algorithms based on the Hough Transform procedure [4]. SIFT [5] and SURF [6] algorithms may have also been suitable to work on this topic. But, on pronotum, the question of how to properly segment the object of interest may have consumed a lot of time to develop or to adapt proper methods. This is why we have turned to way of analyzing images without the need for a segmentation step. The application has been again on beetles images but on *pronotum, head, and body* parts. As the beetles have not been dissected, their anatomical parts have not been set apart. So image segmentation of each part, as they are still attached to the whole specimen, is problematic and has been given up. Coordinates of manual landmarks for each part have been provided and are considered as the ground truth to evaluate the predicted ones by our methods. Fig.1 shows the 8 landmarks that we are looking for.

To achieve the landmarks prediction, a CNN model [7] has been designed using Lasagne library [8]. From a first model version, the network has been trained from scratch on the dataset of pronotum images. In a second step, the training has been modified to include a fine-tuning [9] stage.

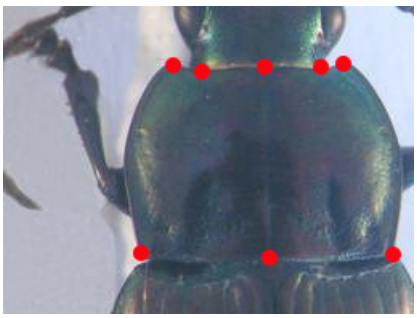

Figure 1: An example of pronotum images and its manual landmarks

In the next section, we present related works about automatic estimation landmarks on 2D images. In section 3, we present the architecture of the network and the procedure to enlarge the dataset. In section 4 we compare the results obtained with the first model and these ones after fine-tuning.

2 Related works

Deep Learning models are coming from machine learning theory. They have been introduced in the middle of previous century for artificial intelligence applications but they encounter several problems to take real-world cases. More recently, the improvement of computing capacities, both in memory size and computing time with GPU programming has opened new perspective for Deep Learning. Many deep learning architectures have been proposed to solve the problems of classification [10, 11], image recognition [12, 13, 14], speech recognition [15, 16] and language translation [17, 18]. To implement the algorithms, many frameworks have been built such as Caffe [19], Theano [20], Tensorflow [21],.... These frameworks help the users to design their application by re-using already proposed network architectures. In image analysis domain, Deep Learning, specifically with CNN, can be used to predict the key points in an image. Yi Sun et al. [22] have proposed a cascaded convolutional network to predict the key points on the human face. Zhang et al. [23] optimize facial landmarks detection with a set of related tasks such as head pose estimation, age estimation, ... Cintas et al. [2] have introduced a network to predict the landmarks on human ear images to characterize ear shape for biometric analysis.

In geometric morphometry, landmarks (or points of interest) are important features to describe a shape. Depending on the difficulty to segment the objects inside the images, setting automatic landmarks can rely on different methods. When segmentation can be applied, Lowe et al. [5] have proposed a method to identify the key points in the 2D image. From the detected key points, the method is able to match two images. Palaniswamy et al. [4] have applied probabilistic Hough Transform to automatically estimate the landmarks in images of Drosophila wings. In a previous study [3], we have extended Palaniswamy's method to detect landmarks automatically on beetles mandibles with good results. Unfortunately, when the segmentation is not precise, we have observed that the results are getting worse. This is why we have turned our work on Deep Learning algorithms in order to find a suitable solution to predict the landmarks without any segmentation step.

3 Network model

Deep Learning is a learning method with multiple levels of representation of connected layers. Data representation is transformed from a lower level to a higher one with many complex functions that can be learned via backpropagation. In this section, we present the initial version of the CNN model that we have used to begin the landmarks prediction.

3.1 Network architecture

The first step to work with CNN is to define the network architecture. After several tests, we have chosen to work with a model provided in Lasagne framework [8] coming from Theano [20]. We will first present the original model and then, we will describe how we have improved it by definition of an *elementary block* that we compose in the final model.

Like the networks have been proposed by Cintas et al. [2], Li et al. [14], and LeCun et al. [7], the proposed network consists of common layers with different learnable parameters. It receives an input image with the size $1 \times 256 \times 192$ to train, to validate, and to test. The network consists of three repeated structures of a convolutional layer followed by a pooling layer (keeping the maximum value). The depth of the convolutional layers increases with the different sizes of the filter kernels (i.e, $2 \times 2, 3 \times 3$). All the kernels of pooling layers have the same size (i.e, 2×2). In the end, three full connected layers are added to the network. The output of the last full-connected layer corresponds to the 16 values which are the 2-coordinates (x, y) of the 8 landmarks to predict.

Experiments with this original model show that this architecture is still not good enough to predict the landmark positions precisely. For instance, overfitting appears during training and validation steps. Srivastava et al. [24] suggest to use dropout sequence to correct overfitting artifacts. Dropout step randomly drops units from the neural network during training and so includes some variations between the different runs. We have updated the model architecture in that way. An *elementary block* is defined as a sequence of convolution (C_i), pooling (P_i) and dropout(D_i) layers that can be repeated several times before to achieve the computation with the full-connected layers. For our purpose, we have assembled 3 *elementary blocks* in our model (see Fig.2). The parameters for each layer are as below, the list of values follows the order of *elementary blocks*:

- CONV layers:
  - Number of filters: $32, 64$, and 128,
  - Kernel filters size: (3×3), (2×2), and (2×2),
  - Stride values: $1, 1, 1$,
  - No padding is used for CONV layers.
- POOL layers:
  - Kernel filters size: (2×2), (2×2), and (2×2),
  - Stride values: $2, 2, 2$.
  - No padding is used for POOL layers.
- DROP layers:
  - Probabilities: $0.1, 0.2$, and 0.3.

In the last full-connected layers (FC), the parameters are: FC1 output: 1000, FC2 output: 1000, FC3 output: 16. As usual, a dropout layer is inserted between FC1 and FC2 with a probability equal to 0.5.

During training, the values of learnable parameters have been updated to increase the accuracy of the network by applying gradient descent in backward phase. Therefore, the network is designed with a small sharing learning rate and momentum. Their values are updated over training time to fit with

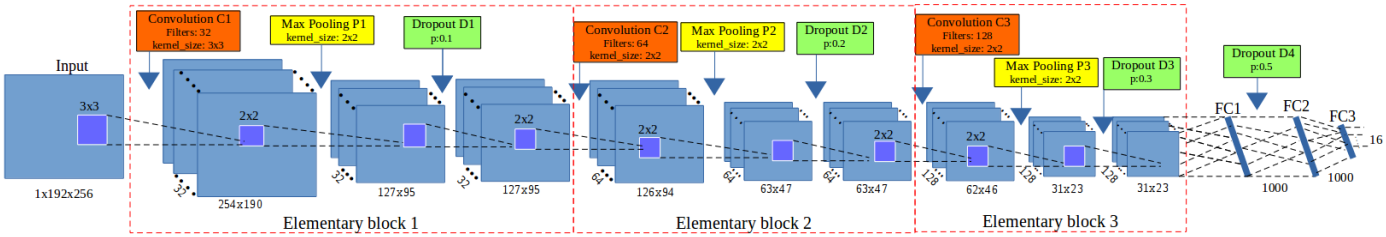

Figure 2: Network architecture using 3 *elementary blocks*. Convolution layer in red, pooling in yellow and dropout in green color.

the number of epochs[1]. The network is designed to finish the training in $5,000$ epochs. The learning rate is initialized at 0.03 and stopped at 0.00001, while the momentum is updated from 0.9 to 0.9999.

The implementation of the network has been done on Lasagne framework [8] which allows computing on GPU. The network has been trained on NVIDIA TITAN X cards.

3.2 Data augementation

The dataset includes 293 images of beetles (for each anatomical part). All images are taken with the same camera in the same condition with a resolution of 3264×2448. Each image has the manual landmarks setting by biologists, i.e, pronotum has 8 manual landmarks. The experiments have been designed with a testing set which includes 33 images randomly chosen and the remained 260 images are used to train and to validate the model. The images in training and validation sets will be chosen randomly followed the ratio during setup the network. For performance considerations, in most of CNNs [7, 22, 10, 2], the size of the input is limited to 256×256 pixels, thus we did down-sampling our images to a new resolution 256×192 (to respect the ratio between x and y), of course the coordinates of manual landmarks have been also scaled to fit with the new resolution.

One of the main characteristics of CNN is that it must use a huge number of data and one can consider that only several hundreds of images is not enough to feed a CNN. Moreover, working with small dataset can push us again to the popular problem of *overfitting*. A way to enlarge the dataset size has to be considered. In image processing, we usually apply transform procedures (translation, rotation) to generate a new image. Unluckily the methods to compute features through a CNN most often are translation and rotation independent. Another way to enlarge the dataset has to be imagined.

A first procedure has been applied to change the value of each color channel in the original image. According to that, a constant is added to one of the RGB channels each time it is used for training. Each constant is sampled in a uniform distribution $\in [1, N]$ to obtain a new value caped at 255. For example, we can add a constant $c = 10$ to the red channel of all images in order to generate new images. This operation can be done for the three color channels.

The second procedure separates the channels of RGB into three gray-scale images. As the network works on single channel images we are able to generate six versions of the same image, the total number of images used to train and to validate is $260 \times 7 = 1820$ images (six versions and original image). This has been an efficient way to proceed to the dataset expansion.

3.3 First results

The set of images that have been used for both training and validation has been built randomly from the original dataset with a ratio of 60% for training and 40% for validation. The training step takes into account a pair of information *(image, manual landmark coordinates)*. At the test phase, images without landmarks are given to the previously trained network to produce output coordinates of the predicted landmarks. To obtain a fast convergence during the computing of CNN, it is useful to normalize the pixel color value between $[0; 1]$ range and the coordinate values have also been normalized [25].

In order to test predictions for all pronotum images (instead of only 33 images), we have applied *cross-validation* to choose the test images. For each time, we have chosen a different fold of 33 images as testing images, called *round*; the remaining images have been used as training and validation images. Following that, the network will be trained with many different training datasets and the output model will be used to predict the landmarks on the images in the corresponding test set. After 9 rounds all images have been tested. Table.1 resumes the training losses for the 9 rounds.

Round	Training loss	Validation loss
1	0.00018	0.00019
2	0.00019	0.00021
3	0.00019	0.00026
4	0.00021	0.00029
5	0.00021	0.00029
6	0.00019	0.00018
7	0.00018	0.00018
8	0.00018	0.00021
9	0.00020	0.00027

Table 1: The losses during training the model on pronotum images dataset

The main goal of the computing is to predict the position of landmarks so the distance (in pixels) between the manual ones (the ground truth) and the predicted ones has to be now

[1] An epoch is a single pass through the full training set.

considered. A correlation test gives us a good correlation between the position of a manual landmark and its corresponding predicted one. But we have considered that this measure is not good enough to provide a useful result to biologists. We have preferred to evaluate the distance in pixels between the ground truth and the prediction. Table.2 shows the average distance between manual and predicted landmarks for all images, landmark per landmark. With images of 256×192 size, we can consider that an error of 1% corresponds to 2 pixels that could be an acceptable error. Unhappily, our results exhibit average distance of 4 pixels in the best case, landmark 1 and more than 5 pixels, landmark 6. Other error distances are more than 2% pixels.

#Landmark	Distance	#Landmark	Distance
1	4.002	5	4.2925
2	4.4831	6	5.3631
3	4.2959	7	4.636
4	4.3865	8	4.9363

Table 2: The average error distance per landmark

To illustrate this purpose, Fig.3 shows the predicted landmarks on two test images. One can note that even some predicted landmarks (Fig.3a) are closed to the manual ones, in some case (Fig.3b) the predicted ones are far from the expect results. The next step has been dedicated to the improvement of these results.

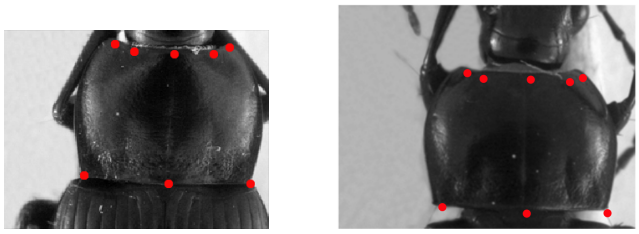

(a) Image with well-predicted landmarks

(b) Image with inaccuracy landmarks

Figure 3: The predicted landmarks, in red, on the images in test set.

4 Fine-tuning to transfer learning

The proposed network presented in section 3.3 has been trained from scratch on the pronotum dataset. As we have discussed, even the statistic test validates the results, when the predicted landmarks are displayed on the image, the results are not enough precise since the average error is still high (≥ 4 pixels).

In order to reach more acceptable results for biologists, we have broadened the model with a step of transfer learning. That is a method that re-uses model developed for a specific task/dataset to lead another task (called *target task*) with another dataset. This allows rapid progress and improves the performance of the model on the target task [26]. The most popular example has been given with the project ImageNet of Google [27] which has labeled several millions of images. The obtained parameter values which can be used in another context to classify another dataset, eventually very different dataset [28]. The name of this procedure to re-use parameters to pre-train a model is currently called *fine-tuning*.

Fine-tuning does not only replace and retrain the model on the new dataset but also fine-tunes the weights of a trained model by continuing the backpropagation. Unfortunately, some rapid tests have shown that re-using ImageNet features has not been relevant for our application. We have designed a way to reproduce the method with our own data. It is worth that of course the size of data to pre-train has drastically decreased. For our pre-training step, the network has been trained on the whole dataset including the images of three parts of beetle i.e pronotum, body and head. Then, the trained model will be used to fine-tune and test on pronotum set.

4.1 Training data preparation

As we have mentioned, the training dataset includes a combination of the images from three sets: pronotum, body, and head (Fig.4). For each set, 260 original images have been chosen randomly for training and validation. By applying the same procedure in section 3.2, the training dataset was enlarged to $5,460$ images ($260 \times 7 \times 3$). However, the number of manual landmarks on each part is different: 8 *landmarks on pronotum part,* 11 *landmarks on body part, and* 10 *landmarks on head part* (Fig.4). The manual landmarks have a specific meaning for the biologists. So, we cannot insert the landmarks arbitrary. Instead of to do that, we keep the smallest number of landmarks among the three parts and remove the supernumerary when it is needed. Specifically, we have removed three landmarks on the body part ($1^{st}; 6^th; 9^{th}$) and two landmarks on the head part ($5th; 6^{th}$) (Fig.4).

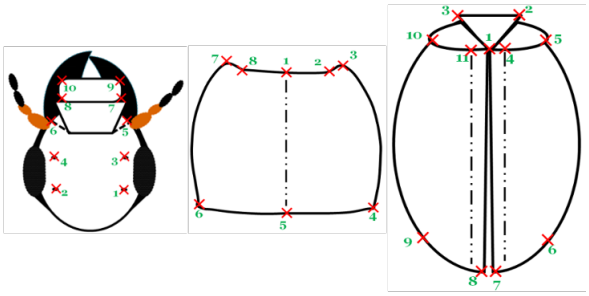

Figure 4: A presentation of head, pronotum and body part with corresponding manual landmarks

4.2 Using fine-tuning for pronotum dataset

At the first step, the network is trained with $5,460$ images following the same way than explained in Section 3.1. After that, this trained model is used to fine-tune the pronotum dataset. To compare the result with the previous one, the trained model has been fine-tuned on pronotum images with different cross-validation (as described in section 3.3). The losses during fine-tuning are shown in Table.3. Comparing with the losses

when we trained the model from scratch (Table.1), the validation losses of this scenario have been significantly improved (around 40%).

Round	Training loss	Validation loss
1	0.00019	0.00009
2	0.00018	0.00010
3	0.00018	0.00010
4	0.00019	0.00008
5	0.00019	0.00009
6	0.00018	0.00008
7	0.00019	0.00008
8	0.00018	0.00006
9	0.00018	0.00009

Table 3: The losses during fine-tuning model

At the end, predicted landmarks are given for the test images. The average error based on the distance between predicted and corresponding manual landmarks has been also computed. The results are shown in Table.4. The **Average** *from scratch* column reminds the average distance obtained previously. The **Average** *with fine-tuning* column presents the new average distance after fine-tuning the pronotum from the trained model. Besides, the standard errors of both cases have been presented (SD columns). It is clearly shown that the result of predicted landmarks with the help of fine-tuning is more precise than the first way to do it.

Landmark	From scratch		With fine-tuning	
	Average	SD	Average	SD
LM1	**4.002**	**2.5732**	**2.486**	**1.5448**
LM2	4.4831	2.7583	2.7198	1.7822
LM3	4.2959	2.7067	2.6523	1.8386
LM4	4.3865	3.0563	2.7709	1.9483
LM5	4.2925	2.9086	2.4872	1.6235
LM6	**5.3631**	**3.4234**	**3.0492**	**1.991**
LM7	4.636	2.8426	2.6836	1.7781
LM8	4.9363	3.0801	2.8709	1.9662

Table 4: A comparing between the average error distances, the standard deviation values per landmark of two steps.

To illustrate the final results, we display the distribution of the distance of both the best and the worst results (resp. landmark 1 and 6). The Fig.5 shows in (a) and (b) diagrams how much the average distances (blue lines) and standard errors (red lines) have been improved for the landmark 1, the (c) and (d) diagrams for the landmark 6.

As a result of working, the program outputs the predicted landmarks of the images as TPS files. With the outputs are TPS files, the user can use MAELab framework[2] to display the landmarks on the images.

[2]MAELab is a free software written in C++. It can be directly and freely obtained by request at the authors.

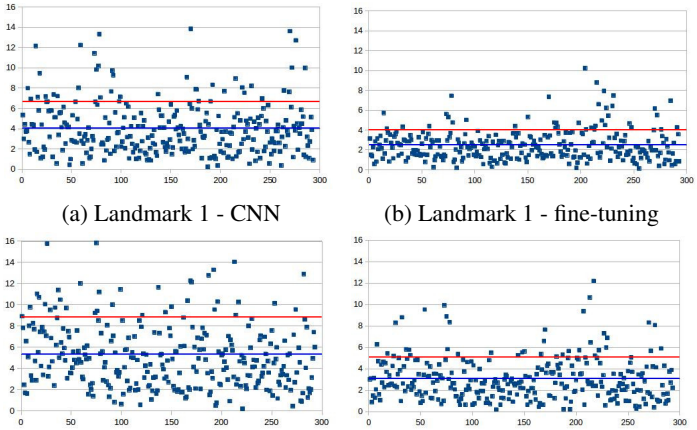

(a) Landmark 1 - CNN (b) Landmark 1 - fine-tuning

(c) Landmark 6 - CNN (d) Landmark 6 - fine-tuning

Figure 5: The distribution of distance error on 1^{st} and 6^{th} landmarks of all images in two testing steps (CNN and fine-tuning). The blue and red lines present the average distances and standard deviation values, respectively.

5 Conclusion

In this paper, we have proposed a CNN model to predict the landmarks on 2D biological images of beetles. The CNN network has been designed from an elementary block repeated three times. This elementary block consists of a convolutional, a max pooling, and a dropout layer. Finally, the elementary blocks are followed after by the usual full connected layers.

In the first step, the model has been trained from scratch and tested on the dataset of pronotum images. In order to improve the results, the model has been trained on a dataset including the images of all three parts of beetles. Then, the trained model has been used to fine-tune and to test on pronotum images.

The results have been evaluated by comparing the coordinates between predicted and manual landmarks. These results have shown that using the convolutional network to predict the landmarks on biological images leads to provide satisfying results without need of segmentation step on the object of interest. The best set of estimated landmarks has been obtained after a step of fine-tuning using the whole set of images that we have for the project, i.e. about all beetle parts. The quality of prediction allows using automatic landmarking to replace the manual ones. In future works, we plan to study more deeply how to characterize the learning problem to design the right pre-training set.

Acknowledgements

The research has been supported by DevMAP project[3]. We would like to thank our colleague, ALEXIA Marie, who have provided manual landmarks on beetle images.

[3]https://www6.rennes.inra.fr/igepp_eng/Research-teams/Demecology/Projects/INRASPEDevMAP

References

[1] A. Sonnenschein *et al.*, "Supporting material and data for "an image database of drosophila melanogaster wings for phenomic and biometric analysis"," 2015.

[2] C. Cintas *et al.*, "Automatic ear detection and feature extraction using geometric morphometrics and convolutional neural networks," *IET Biometrics*, vol. 6, no. 3, pp. 211–223, 2016.

[3] V. L. Le, M. Beurton-Aimar, A. Krahenbuhl, and N. Parisey, "MAELab: a framework to automatize landmark estimation," in *WSCG 2017*, (Plzen, Czech Republic), May 2017.

[4] S. Palaniswamy, N. A. Thacker, and C. P. Klingenberg, "Automatic identification of landmarks in digital images," *IET Computer Vision*, vol. 4, no. 4, pp. 247–260, 2010.

[5] D. G. Lowe, "Distinctive image features from scale-invariant keypoints," *International journal of computer vision*, vol. 60, no. 2, pp. 91–110, 2004.

[6] H. Bay, T. Tuytelaars, and L. Van Gool, "Surf: Speeded up robust features," in *European conference on computer vision*, pp. 404–417, Springer, 2006.

[7] Y. LeCun, K. Kavukcuoglu, and C. Farabet, "Convolutional networks and applications in vision," in *Circuits and Systems (ISCAS), Proceedings of 2010 IEEE International Symposium on*, pp. 253–256, IEEE, 2010.

[8] S. Dieleman *et al.*, "Lasagne: First release.," Aug. 2015.

[9] J. Yosinski, J. Clune, Y. Bengio, and H. Lipson, "How transferable are features in deep neural networks?," in *Advances in neural information processing systems*, pp. 3320–3328, 2014.

[10] A. Krizhevsky, I. Sutskever, and G. E. Hinton, "Imagenet classification with deep convolutional neural networks," in *Advances in neural information processing systems*, pp. 1097–1105, 2012.

[11] D. Ciregan, U. Meier, and J. Schmidhuber, "Multi-column deep neural networks for image classification," in *Computer Vision and Pattern Recognition (CVPR), 2012 IEEE Conference on*, pp. 3642–3649, IEEE, 2012.

[12] C. Szegedy *et al.*, "Going deeper with convolutions," Cvpr, 2015.

[13] C. Farabet, C. Couprie, L. Najman, and Y. LeCun, "Learning hierarchical features for scene labeling," *IEEE transactions on pattern analysis and machine intelligence*, vol. 35, no. 8, pp. 1915–1929, 2013.

[14] H. Li, Z. Lin, X. Shen, J. Brandt, and G. Hua, "A convolutional neural network cascade for face detection," in *Proceedings of the IEEE Conference on Computer Vision and Pattern Recognition*, pp. 5325–5334, 2015.

[15] T. Mikolov *et al.*, "Strategies for training large scale neural network language models," in *Automatic Speech Recognition and Understanding (ASRU), 2011 IEEE Workshop on*, pp. 196–201, IEEE, 2011.

[16] G. Hinton *et al.*, "Deep neural networks for acoustic modeling in speech recognition: The shared views of four research groups," *IEEE Signal Processing Magazine*, vol. 29, no. 6, pp. 82–97, 2012.

[17] S. Jean, K. Cho, R. Memisevic, and Y. Bengio, "On using very large target vocabulary for neural machine translation," *arXiv preprint arXiv:1412.2007*, 2014.

[18] I. Sutskever, O. Vinyals, and Q. V. Le, "Sequence to sequence learning with neural networks," in *Advances in neural information processing systems*, pp. 3104–3112, 2014.

[19] Y. Jia *et al.*, "Caffe: Convolutional architecture for fast feature embedding," *arXiv preprint arXiv:1408.5093*, 2014.

[20] Theano Development Team, "Theano: A Python framework for fast computation of mathematical expressions," *arXiv e-prints*, vol. abs/1605.02688, May 2016.

[21] M. Abadi *et al.*, "TensorFlow: Large-scale machine learning on heterogeneous systems," 2015. Software available from tensorflow.org.

[22] Y. Sun, X. Wang, and X. Tang, "Deep convolutional network cascade for facial point detection," in *Proceedings of the IEEE conference on computer vision and pattern recognition*, pp. 3476–3483, 2013.

[23] Z. Zhang *et al.*, "Facial landmark detection by deep multi-task learning," in *European Conference on Computer Vision*, pp. 94–108, Springer, 2014.

[24] N. Srivastava, G. E. Hinton, A. Krizhevsky, I. Sutskever, and R. Salakhutdinov, "Dropout: a simple way to prevent neural networks from overfitting.," *Journal of machine learning research*, vol. 15, no. 1, pp. 1929–1958, 2014.

[25] Y. A. LeCun *et al.*, "Efficient backprop," in *Neural networks: Tricks of the trade*, pp. 9–48, Springer, 2012.

[26] L. Torrey and J. Shavlik, "Transfer learning," *Handbook of Research on Machine Learning Applications and Trends: Algorithms, Methods, and Techniques*, vol. 1, p. 242, 2009.

[27] J. Deng *et al.*, "ImageNet: A Large-Scale Hierarchical Image Database," in *CVPR09*, 2009.

[28] J. Margeta *et al.*, "Fine-tuned convolutional neural nets for cardiac mri acquisition plane recognition," *Computer Methods in Biomechanics and Biomedical Engineering: Imaging & Visualization*, vol. 5, no. 5, pp. 339–349, 2017.